Lab on a Chip

Accepted Manuscript

ROYAL SOCIETY OF CHEMISTRY

www.rsc.org/loc

Graphical Abstract

Electrospun TiO_2-Nanofibers Integrated Lab-on-a-Disc for Ultrasensitive Protein Detection from Whole Blood

Won Seok Lee,‡ Vijaya Sunkara,‡ Ja-Ryoung Han, Yang-Seok Park, Yoon-Kyoung Cho*

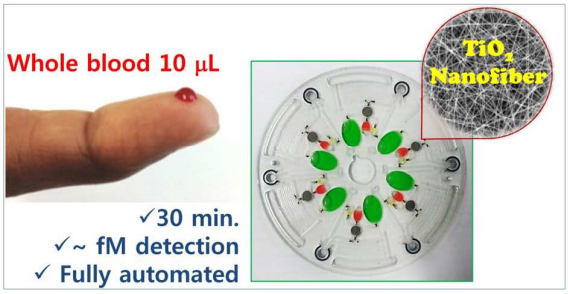

From 10 μL of whole blood, full steps of an ELISA are automated to achieve femtomolar- and picomolar-level detection for C-reactive proteins and cardiac troponin I respectively.

Cite this: DOI: 10.1039/c0xx00000x

www.rsc.org/xxxxxx

ARTICLE TYPE

Electrospun TiO_2 nanofibers integrated lab-on-a-disc for ultrasensitive protein detection from whole blood†

Won Seok Lee,‡ Vijaya Sunkara,‡Ja-Ryoung Han, Yang-Seok Park, Yoon-Kyoung Cho*

Received (in XXX, XXX) XthXXXXXXXXX 20XX, Accepted Xth XXXXXXXXX 20XX

DOI: 10.1039/b000000x

ELISA based devices are promising tools for the detection of low abundant proteins in biological samples. Reductions of the sample volume and assay time as well as full automation are required for its potential use in point-of-care diagnostic applications. Here, we present a highly efficient lab-on-a-disc composed of TiO_2nanofibrous mat for sensitive detection of serum proteins with a broad dynamic range, with only 10 μL of whole blood within 30 min. The TiO_2 nanofibers provide high specific surface area as well as active functional groups to capture large amounts of antibodies on the surface. In addition, the device offers efficient mixing and washing for improving the signal to noise ratio, thus enhancing the overall detection sensitivity. We employ the device for the detection of cardiac biomarkers, C-reactive protein (CRP) and cardiac troponin I (cTnI), spiked in phosphate buffered saline (PBS) as well as in serum or whole blood. The device exhibited a wide dynamic range of six orders of magnitude from 1 pg mL^{-1} (~8 fM) to 100 ng mL^{-1} (~0.8 pM) and a low detection limit of 0.8 pg/mL (~6 fM) for CRP spiked in CRP free serum and a dynamic range from 10 pg mL^{-1} (~0.4 pM) to 100 ng mL^{-1} (~4 nM) with a detection limit of 37 pg/mL (~ 1.5 pM) for cTnI spiked in whole blood.

Introduction

Rapid and sensitive detection of biomarkers allows early disease diagnosis, treatment monitoring and better management of various diseases. Though the enzyme-linked immunosorbant assay (ELISA) is a gold standard method for the detection of the protein biomarkers in biological samples, its low sensitivity deters the diagnosis at an early stage of the disease. Furthermore, large amount of required sample volumes, relatively long assay time and lack of automation have been bottlenecks for broader applications such as point-of-care devices for monitoring disease progression and evaluating therapeutic responses. Therefore, design and development of highly sensitive devices to detect the low abundant biomarkers in small volume of samples is an issue of vital importance. To address this issue, various nanoscale materials[1,2] such as nanoparticles (NPs),[3] nanotubes (NTs),[4] nanowires (NWs),[5] and nanofibers (NFs)[6-8] have been utilized in the design of highly sensitive biosensors. Due to the intriguing physico-chemical properties and high surface to volume ratio, the nanoscale materials show superior detection sensitivities. For example, a microfluidic immunoassay for human immunodeficiency virus (HIV) on a polycarbonate NFs membrane prepared by electrospinning showed dramatic improvement in sensitivity and signal-to-noise ratio compared with that on the plain substrates.[7]

In recent years, the electrospun NFs are receiving great attention because of their simple and cost-effective fabrication process as well as their high specific surface area.[9,10] The electrospinning technique has the ability to fabricate ultra-long NFs of a desired size from nanometer to sub-micrometer diameter with relatively simple instruments.[11] In addition, the diameter of the NFs can be tuned by changing a few operating conditions such as the applied voltage, the flow rate, and/or the concentration of the precursor solution. Normally, the structure of the collected NFs is random, however, they can be easily aligned on demand for various applications.[12] The NFs can be fabricated with various polymers such as polycarbonate,[7] polystyrene[13] etc. However, the polymer NFs suffers from the difficulties in handling, modification and covalent immobilization of antibodies on the surface. Therefore, there is a critical need for a versatile and robust material that can be easily functionalized with the target specific antibodies.

Recently, Titanium dioxide (TiO_2)-based nanomaterials have been proposed as excellent candidates for biosensing,[8,14,15] as they display remarkable properties such as chemical stability,[16] negligible protein denaturation,[17] biocompatibility,[18] and more importantly the versatility in functionalization.[19,20] The TiO_2 NFs can be easily fabricated by electrospinning.[21] However, the high-density NF mat formed after calcination is brittle and difficult to integrate into a device. Hence, it is rare that the high-density electrospun NFs are employed in bio-analysis applications despite of their great advantages. Therefore, it is highly desirable to have a method that integrates the brittle NF mat onto the target device for broad applications. Here, we have developed a technology that can transfer electrospun NF mats to any target surface using a thin polydimethylsiloxane (PDMS) adhesive layer. Furthermore, integration and automation of all the functions including separation, metering, mixing, washing, and detection

into one single device can greatly simplify the immunoassay process. For this purpose, lab-on-a-disc was developed as a point-of-care analytical device to allow chemical and/or biological assays outside of laboratory environments.[22,23] We have previously demonstrated that ELISAs can be performed in a fully automated manner on a disc starting from whole blood.[24-26] Instead of multiple syringe pumps and tubing connections, a single motor is utilized to transfer multiple types of reagents preloaded on a disc.

In the present work, a high-density TiO_2 electrospun NF mat transferred and assembled onto a PC disc utilizing a thin PDMS adhesive layer was used as a solid substrate for the ultrasensitive immunoassay. In addition, the distinct characteristics of TiO_2 were exploited to prepare functionalized NFs that were derivatized to covalently bind the monoclonal antibodies. Here, the unique ability of the antibody coated NFs to specifically recognize its antigen combined with the effective mixing and washing on the lab-on-a-disc platform provides ultrasensitive detection system for low abundant biomarkers.

Materials and Methods

Materials

Titanium tetraisopropoxide (TTIP, 98%, Aldrich), polyvinylpyrrolidone (PVP, Mw = 1,300,000), acetic acid, anhydrous ethanol (99.5%), and tridecafluoro-1,1,2,2-tetrahydrooctyl)-1-trichlorosilane were purchased from Sigma-Aldrich. The PDMS pre-polymer (Sylgaurd 184) and curing agents were from Dow Corning, GPDES was purchased from Gelest Inc., and the chemiluminescent substrate (SuperSignal® ELISA Femto) was from Invitrogen; Blood was obtained from healthy donors and was collected in K2 EDTA tubes (BD vacutainer, K2 EDTA 7.2 mg plus blood collection tubes). Written informed consent was obtained from all volunteers. All other chemicals and materials were purchased from local vendors.

Fabrication of TiO_2 NFs

Fabrication of TiO_2 NFs includes three steps: 1) synthesis of the precursor solution, 2) electrospinning, and 3) the calcination process. The process is as follows. First, the precursor solution was prepared by dissolving TTIP (1.5g) in ethanol (3 mL)/acetic acid (3 mL), and a solution containing 11-wt% PVP in ethanol was then added to the solution and mixed thoroughly. Second, the PVP/TTIP NFs were fabricated by using an electrospinning method in which the solution was constantly introduced through a stainless-steel needle at a flow rate of 0.3 mL h^{-1} onto a Si wafer (2 cm × 2 cm) placed on a grounded substrate at a high DC voltage (15 kV) and at a fixed distance of 10 cm between the needle and the grounded substrate. Third, the PVP/TTIP NFs on the Si wafer were calcinated at 500°C for 3 h under high-vacuum conditions (5×10^{-5}Torr).Field-emission scanning electron microscopy (FE-SEM, FEINano230), high-resolution transmission electron microscopy (HR-TEM, JEM-2100F), and energy dispersive spectrometry (EDS, JEM-2100F) were used for the analyses of the electrospun TiO_2 NFs.

Fabrication of a centrifugal microfluidic disc

The details of disc fabrication and valve formation were reported elsewhere.[27] In brief, microfluidic channels and chambers were fabricated on the bottom PC disc (5 mm thick) of 12 cm diameter by CNC micromachining (3D modeling machine; M&I CNC Lab, Korea). The injection holes were fabricated on the top disc, and ferrowax was printed on the loading chambers by using a custom-designed wax-dispensing machine (Hanra Precision Eng. Co. Ltd., Korea). Before bonding the two plates, a TiO_2 NF mat was integrated into the binding reaction chambers, and antibodies were then immobilized on the TiO_2 NFs. The top and bottom plates were bonded by using double-sided adhesive tape (DFM 200 clear 150 POLY H-9 V-95, FLEXcon, USA), which was prepared by a cutting plotter (Graphtec CE3000-60 MK2, Graphtec Corporation, Japan).

Transfer of the NF mat onto the target substrates

Silicon substrates: The PDMS pre-polymer was mixed with a curing agent at a 10:1 ratio, degassed, and spin-coated onto a silicon substrate at 3000 rpm for 60 s to obtain a 20-μm-thick layer. This was cured in a hot-air oven at 65°C for 4 min. The TiO_2 NF mat fabricated by electrospinning and calcination was transferred onto the PDMS-coated silicon, and the silicon substrate was then incubated in an oven at 65°C for 4 h or at 80°C for 1 h to completely cure the PDMS.

Lab-on-a-disc: A silicon substrate was silanized with tridecafluoro-1,1,2,2-tetrahydrooctyl)-1-tri-chlorosilane under vacuum conditions for 30 min. The PDMS pre-polymer was mixed with a curing agent at a 10:1 ratio, degassed, and spin-coated onto the silanized silicon substrate at 650 rpm for 60 s to obtain a 100-μm-thick layer. This was pre-cured in a hot-air oven at 65°C for 10 min. The TiO_2 NF mat fabricated by electrospinning and calcination was transferred onto the PDMS-coated silicon. After transfer, TiO_2 on the PDMS layer was cut using a punch hole of 6 mm diameter, and the disc of TiO_2 NFs on the PDMS layer was then transferred to the binding reaction chambers in a centrifugal microfluidic disc, where the binding reaction chambers were pre-coated with 20 μL of PDMS pre-polymer. Here, the PDMS pre-polymer acts as an adhesive layer to rigidly attach the disc of TiO_2 NFs onto PDMS. Finally, the centrifugal microfluidic disc was incubated in an oven at 65°C for 4 h or at 80°C for 1 h to completely cure the PDMS.

Surface modification and immunoassay

GPDES reaction: The TiO_2 NF mat was treated with oxygen plasma (140 W, 50 sccm, and 180 s), and immersed in 1% v/v solution of GPDES in ethanol, incubated for 2 h at RT. 1-20 mL of the solution was used per substrate depending on the size of the substrate. The substrates were washed briefly with ethanol, cured at 80°C for 1 h, sonicated in ethanol for 10 s to remove the physically adsorbed and unbound GPDES molecules, washed again with ethanol, blown dry with a nitrogen stream, dried under vacuum, and stored in a sealed container at RT until use.

Immobilization of antibodies on the surface: The concentrations of the capture antibody and secondary antibody were optimized on the basis of the S/N ratio of the signals obtained at various concentrations. The optimal concentration of the capture antibody

required to coat the TiO_2 NF was found to be 200 μg/mL for both CRP and cTnI, and the optimal concentration of the secondary antibody was found to be 400 ng/mL for CRP and 1 μg/mL for cTnI. A solution of 200 μg/mL of capture antibodies was made by diluting the antibodies with a phosphate buffered saline (PBS) buffer (pH 7.4), and 5 μL of the solution was dispensed onto each substrate using a micropipette. The substrates were kept in a humidified chamber and incubated at 37°C for 4 h. They were then washed with the 0.1% BSA–PBS buffer, incubated with the 1% BSA–PBS buffer at 37°C for 1 h to block the un-reacted sites, and subsequently washed twice with 0.1% BSA–PBS. The substrates were dipped in the 0.1% BSA–PBS buffer at 4°C and stored at these conditions until use. Same procedure was applied for the surface modification of NFs integrated on a disc, before bonding the top and bottom plates. The presence of anti-CRP antibodies and the CRP on the TiO_2 NF mat was characterized by X-ray photoelectron spectroscopy (XPS, K-alpha).

On-disc immunoassay: First, 10 μL of antigen-spiked whole blood was loaded on the disc using a micro pipette and the disc was spun at 3600 rpm for 60 s to separate the red blood cells. Next, valve #1 was opened by laser irradiation, and 4 μL of the supernatant plasma was transferred to the chamber containing 8 μL of detecting antibodies conjugated with HRP by spinning the disc in a mixing mode for 5 s. The cycle of acceleration and deceleration (15 Hz s^{-1}, 15°) was repeated to achieve efficient binding between the protein and the detection antibodies. Then, the mixture was transferred to a binding reaction chamber by opening valve #2 and incubated in a mixing mode (60 Hz s^{-1}, 2°) for 20 min. After the immunoreaction, the residual mixture was removed to the waste chamber by opening valve #3. Then, valve #4 was opened, and the washing buffer solution (600 μL) was transferred to the binding reaction chamber. After washing the TiO_2 NFs in a mixing mode (30 Hz s^{-1}, 30°), the waste solution was transferred to the waste chamber. This step was repeated two more times, and then, valve #5 was closed. Next, valve #6 was opened to transfer the chemiluminescent substrate solution to the binding reaction chamber and incubated in a mixing mode (30 Hz s^{-1}, 2°) for 1 min. Finally, valve #7 was opened, and the reacted substrate solution was transferred to the detection chamber. The chemiluminescence signals were measured with a home built detection system equipped with a cooled PMT module (PMC-100-1, Becker & Hickl GmbH) (see ESI† Fig. S1).

Off-disc immunoassay: A solution of antigen and secondary antibodies labelled with HRP of desired concentration was prepared using either PBS at a pH of 7.4, a CRP-free serum, or whole blood. A volume of 10μL of this solution was dispensed onto each substrate and incubated for 20 min. The substrates were washed twice with 0.1%BSA–PBS on a plate shaker at 120 rpm for 2 min each. After removing the washing buffer, 110 μL of the chemiluminescent substrate solution was added and incubated with shaking for 1 min. A volume of 100 μL of this solution was transferred to the 96-well opaque microplate, and the relative light units (RLUs) were measured with a modular multilabel plate reader (Perkin Elmer / Envision 2104).

Results and Discussion

Fabrication of TiO_2 nanofibers

A typical electrospinning setup is schematically shown in Fig. 1. The TiO_2 NFs were fabricated by electrospinning a mixture of a polymer and TiO_2 additives followed by a calcination process to decompose the organic components.[21] The electrospinning conditions were optimized on the basis of our requirements. The size and thickness of the TiO_2 NFs were tailored by controlling the flow rate, time, and applied voltage. It was observed that NFs were not formed at a low voltage (5 kV) and broken at a higher voltage (20 kV). Similarly, a higher flow rate resulted in bead formation during electrospinning (see ESI† Fig. S2); thus, an applied voltage of 15 kV and a flow rate of 0.3 mL h^{-1}were selected as the optimum conditions for NF fabrication. After calcination, the thickness of the NF mat was 2 ± 0.5, 30 ± 1, and 90 ± 5 μm from 1, 10, and 30 min of electrospinning, respectively (Fig. 2). Although the thick layer may provide a larger surface area, the NF layer could be detached at the interface between the layers if the mat is too thick. Therefore, 10 min was selected as the optimum time to avoid detachment.

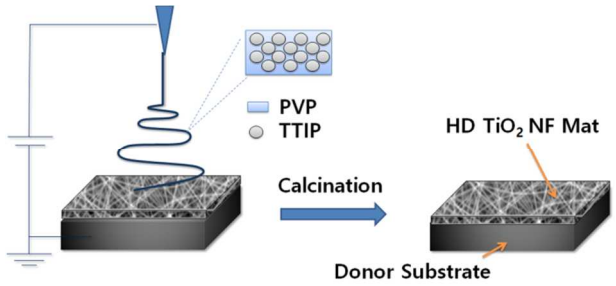

Fig. 1 Schematic diagram showing the fabrication process of TiO_2 NF mat on a donor substrate by electrospinning and calcination.

After calcination, a very thin layer of TiO_2 NFs remains intact on the grounded substrate[8] and the thick TiO_2 NF mat shrinks and could be easily peeled off from the substrate due to the weak adhesion.[28] As the obtained TiO_2 NF mats are brittle, it is very difficult to handle and integrate them with the functional devices. As an effort to solve this problem, a hot-press[29] and solvent–vapor[30] techniques have been developed to enhance the adhesion between the TiO_2/polymer NF mat and the substrate before the calcination step. Although both methods could increase adhesion, they could also ruin the morphology of the TiO_2 NFs. For example, in the hot-press technique, TiO_2 NFs are broken and damaged by the high mechanical pressure, while the shape of the TiO_2 NFs is deformed because of the *N*,*N*-dimethylformamide (DMF) solution used in the solvent–vapor technique. Furthermore, these methods have limited applicability and cannot be used for the integration of NFs on various target substrates that are not compatible with the follow-up calcination step. Here, in order integrate the high-density NF mat to a functional device we have utilized a thin PDMS adhesive layer for transfer printing.

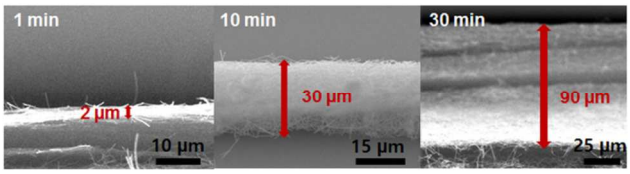

Fig. 2 Thickness of the TiO_2 NF mats prepared with various electrospinning times.

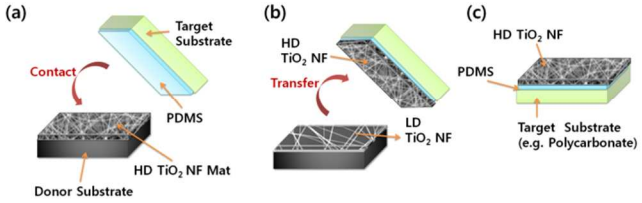

Fig.3 Schematic diagram illustrating the process of a TiO_2 NF mat transferred to a target substrate using a thin adhesive layer of PDMS: (a) transfer printing of the TiO_2 NF mat onto a PDMS-coated target substrate by contact, (b) transferred TiO_2 NF mat on the target substrate with some TiO_2 NFs left on the donor substrate, and (c) TiO_2 NFs assembled on the target device by transfer printing.

Transfer printing of TiO_2 nanofibers mat

The transfer-printing process of a TiO_2 NF mat from a donor substrate to a target substrate coated by a thin PDMS film as an adhesive layer is illustrated in Fig.3. An important variable in the proposed transfer-printing process is the pre-curing condition of the PDMS layer, which plays a major role in the quality of the NFs and influences the final assay results. When the PDMS layer was cured for shorter time, the NF mat became embedded into the PDMS layer. At the same time, the NFs could not adhere strongly and peeled off from the substrate if it was cured too long (see ESI† Fig. S3). A tack test was performed on 100μm-thick PDMS substrates cured for 3, 10, and 30 min to measure the adhesion strength (see ESI† Fig. S4). From the data, the optimal pre-curing time for integrating the TiO_2 NF mat to the PDMS film without detachment or submergence was 10 min. Similarly, it was 4 min for 20-μm-thick PDMS film.

The target substrates with the transferred TiO_2 NF mat and the donor with the remaining TiO_2 NFs were denoted as the high-density (HD) NFs and low-density (LD) NFs, respectively, and used for the immunoassay to compare the effects of surface area. Scanning electron microscopy (SEM) images of TiO_2 NFs fabricated and transfer-printed under optimal conditions are shown in Fig.4a-d. As shown in Fig. 4b and 4d, the TiO_2 NF mat was stably fixed to the target substrate with strong adhesion. The density and thickness of the TiO_2 NF mat on the target substrate are higher compared to the TiO_2 NFs on the donor substrate (Fig. 4c and 4d). The TEM–EDS analysis indicates the presence of O and Ti and the percent compositions in a single electrospun TiO_2NF (see ESI† Fig. S5 and Table S1). The average diameter of the TiO_2 NFs was found to be approximately 100 nm from the data in the histogram (see ESI† Fig. S6).

Surface modification and characterization

In order to increase the accessibility of capturing antibodies immobilized on the NFs to the target analyte, (3-glycidoxypropyl)methyldiethoxysilane (GPDES) was used to functionalize the TiO_2 surface so that the capture antibody could be covalently attached (Fig.5a). The remaining active sites on the surface were blocked with 1% bovine serum albumin (BSA) in a PBS buffer to prevent non-specific binding. The presence of antibodies on the surface and the specific capture of the target protein by the antibody-modified TiO_2 NFs were also examined by X-ray photoelectron spectroscopy (XPS). The spectra were obtained before and after antibody immobilization also after treatment with the target protein (Fig. 5b and see ESI† Table S2). The change in elemental composition after each treatment indicates a change in the functional group on the surface. Appearance of the N1s signal at a binding energy 398–401 eV, corresponding to the N–C, N–C=O and N-H binding states of nitrogen, indicates the presence of the anti-CRP antibodies on the surface, and an increase in its percentage after treatment with the target protein indicates that the protein (CRP) was bound to the surface-tethered antibodies. Similarly, the signal between 286–289 eV, corresponding to C=O and C–O binding states, shows the presence of the antibody on the surface, and an increase in the percentage reveals the target-protein interaction with the surface-bound antibody. In addition, the C 1s signal at binding energy of 282–286 eV, corresponding to C–C and C=C binding states, is due to the carbon formed during the pyrolysis of PVP while fabricating TiO_2 NFs.

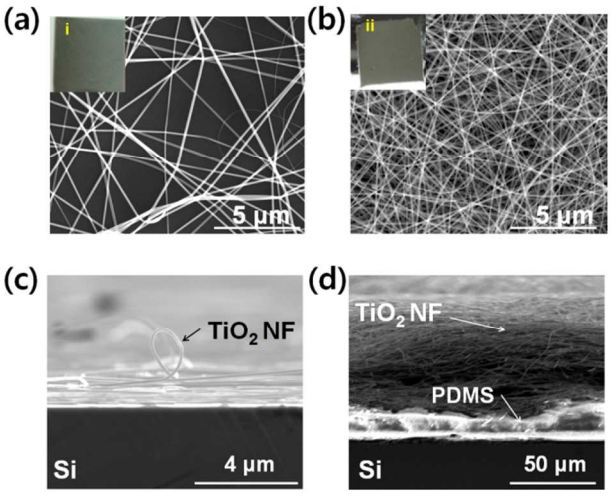

Fig.4 SEM images of the TiO_2 NFs: (a) top and (c) side views of low-density TiO_2 NFs remaining on the donor Si substrate and (b) top and (d) side views of a high-density TiO_2 NF mat transferred to the target Si substrate; insets i and ii are the photographs of the TiO_2 NFs (2 cm × 2 cm).

Immunoassay

As a proof of concept, the assay for CRP and cTnI detection was performed on the TiO_2 NF mat integrated into a lab-on-a-disc, as shown in Fig. 6 (See a movie file in the ESI†). A photograph of the disc containing the HD TiO_2 NF mat coated with the capture antibodies and the chambers for detecting antibodies, the washing buffer, and the chemiluminescent substrate along with a more detailed fluidic layout are shown in Fig. 6a. The valves are laser actuated to control the fluidic transfer, and the details have been reported elsewhere.[27] Fig. 6b shows the ELISA process starting from whole blood. Images were captured by a CCD camera and a strobe light during the spinning of the disc. The spin program is listed in Table S3 in the ESI†. In short, the disc spun at 3600 rpm for 60 s to separate the red blood cells from 10 μL of antigen

spiked whole blood (Fig. 6b-i); after separation, 4 µL of plasma was transferred to a chamber containing 8 µL of detecting antibodies conjugated with horseradish peroxidase (HRP) and mixed with the detection reagents (Fig. 6b-ii). The entire solution was transferred to a binding reaction chamber and incubated with mixing for 20 min (Fig. 6b-iii). The supernatant liquid was removed, and the NFs were washed thrice with a washing buffer (Fig. 6b-iv). After complete removal of the washing buffer, a chemiluminescent substrate solution was transferred to the NFs and then incubated for 1 min (Fig. 6b-v). Finally, the substrate solution was transferred to the detection chamber to measure the luminescence intensity (Fig. 6b-vi).

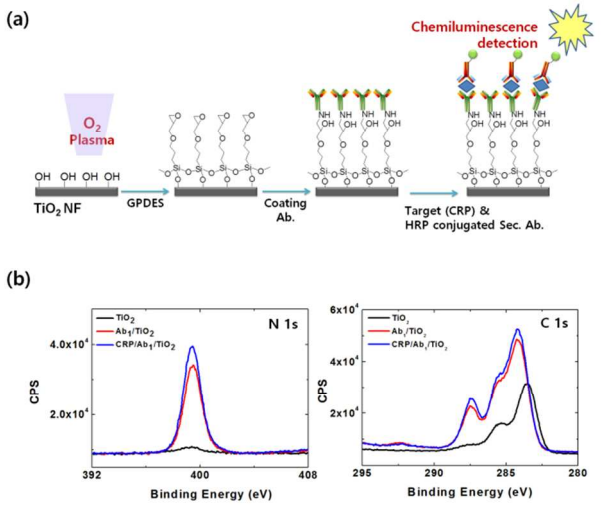

Fig.5 (a) Schematic representation of antibody immobilization and the immunoassay on the TiO_2 NFs. (b) XPS spectra of immobilized anti-CRP and CRP on the surface of TiO_2 NFs showing the N 1s and C 1s peaks.

The off-disc immunoassay was performed on HD and LD TiO_2 NFs and in a 96-well plate. For the NFs, the final analyte solution was prepared by serial dilution of aliquots of CRP for a concentration ranging from 1 pg mL^{-1} to 100 ng mL^{-1} using a CRP-free serum, and a solution of HRP-conjugated secondary antibodies in PBS buffer was added to create the final solution containing a concentration of 400 ng mL^{-1} of secondary antibodies in all CRP aliquots (see ESI† Fig. S7). Similarly, for cTnI, the solutions of concentrations ranging from 10 pg mL^{-1} to 100 ng mL^{-1} of cTnI, containing 1 µg mL^{-1} of secondary antibodies in all cTnI aliquots were prepared using normal sera. A volume of 10 µL of the analyte solution was added to each substrate and incubated for 20 min. For the 96-well plate, the assay was performed with the same antibody sets using a standard protocol (e.g., 100 µL of serum, 4 h of operation time). Here, the CRP free serum was used intentionally in order to demonstrate the low detection limit of the device. Because the CRP levels in healthy sera or whole blood are in microgram range and therefore it is not appropriate to use them for evaluating the limit of detection. Nonetheless, the experiments were conducted using whole blood or healthy sera for the detection of cTnI.

The calibration graphs for the determination of CRP and cTnI were created by plotting the S/N ratio of the RLU versus the analyte concentration and are shown in Fig. 7a for CRP spiked in the CRP-free serum comparing i) the conventional 96-well plate, ii) the LD NF mat on a Si substrate, iii) the HD NF mat assembled on a Si substrate, and iv) the HD NF mat assembled on a lab-on-a-disc and in Fig. 7b for cTnI spiked in whole blood or the PBS buffer comparing HD TiO_2 NFs assembled on a Si substrate, on a lab-on-a-disc, and a 96-well plate. The assay for CRP on TiO_2 NFs exhibited a broad linear dynamic range of six orders of magnitude from 1 pg/mL to 100 ng/mL with a detection limit of 0.8, 2.5, and 8 pg/mL (~6, 20, and 64 fM) for the HD NFs on a disc, the HD NFs on Si, and the LD NFs on Si, respectively (see ESI† Fig. S8). On the other hand, the cTnI assay exhibited a broad linear dynamic ranges of six orders of magnitude in PBS with a detection limit of 4.4 pg/mL for HD NFs on Si and five orders of magnitude in whole blood with a detection limit of 37, 64 and 824 pg/mL for the HD NFs on a disc, the HD NFs on Si, and 96-well plate, respectively (see ESI† Fig. S9).

Here, we demonstrate femtomolar (fM)-level and picomolar (pM)-level detection of CRP and cTnI, respectively, from as little as 10 µL of whole blood by utilizing the novel material properties of electrospun TiO_2 NFs, such as the ultra-high surface area as well as the capability of covalent bonding with antibodies. In previous studies, the substrate material was polystyrene, which is the same as the 96-well plate, and the antibodies were immobilized by physisorption with a random orientation. Now, by taking advantage of the higher surface area, the easy fabrication, and surface modification of the TiO_2 NFs, we could demonstrate CRP and cTnI detection from only 10 µL of whole blood with fM and pM detection sensitivity, respectively, in a fully automated lab-on-a-disc platform.

It is worthwhile to note that the S/N ratio on a disc is higher than the Si substrate. This is because much more efficient washing may be performed on a disc rather than a flat substrate. The efficient washing on a disc helps remove the non-specifically bound molecules, which results in low background and higher signal; thus, the S/N ratio is higher on a disc compared to a Si substrate. The lab-on-a-disc exhibited a higher sensitivity for protein detection, which is approximately three times higher than the off-disc HD NFs, 300 times higher than the conventional ELISA in a 96-well plate for CRP, and approximately two times higher than the off-disc HD NFs for cTnI. This ultrasensitive detection was achieved despite the fact that at least a 25 times smaller sample volume (100 µL versus 4 µL of plasma) was used, and the total assay time was a minimum of eight times shorter (4 h versus 30 min).

Conclusions

The electrospun TiO_2 NFs integrated lab-on-a-disc affords a significant improvement in the sensitivity with a broad dynamic range. The detection limits are ~300 fold lower than the conventional ELISA technique. In addition, the device presents several advantages, including reduced costs, inexpensive equipment, fast analysis and easy handling. Moreover, the method used for integrating the brittle nanofibrous mat into a functional device offers excellent prospects for the design of new technologies. With the proposed method, the electrospun nanomaterials can be transferred onto any substrate including non-conductive and plastic materials; the HD TiO_2 NF mat can be assembled on a local chamber with a high adhesion force, and it

remains stable during the multiple washing steps required for a highly sensitive immunoassay. Therefore, we could successfully transfer the NFs prepared on a silicon substrate to a centrifugal microfluidic disc made of PC. With this transfer-printing technology, one can fully utilize the novel properties of electrospun TiO_2 NF mats, even with devices made of thermoplastics. To the best of our knowledge, this is the first example of the integration and utilization of nanomaterials for the "sample-in and answer-out" type of fully automated immunoassays and the demonstration of an ultrasensitive immunoassay using as little as 10 μL of whole blood. Due to its excellent sensitivity with very low volumes of blood, the device would enable the screening of biomarkers at an early stage of the disease, thus providing improved therapeutic outcomes. Although the detection of cardiac biomarkers was demonstrated as a proof of concept for the performance of the device, it could be adapted for the detection of any biomarker, subject to the availability of its specific antibodies. On top of all, the device provides significant impact on pharmaceutical industry because now, with this device, long-term effects of the drug on test animal, e.g. mouse, could be monitored, without scarifying the animal.

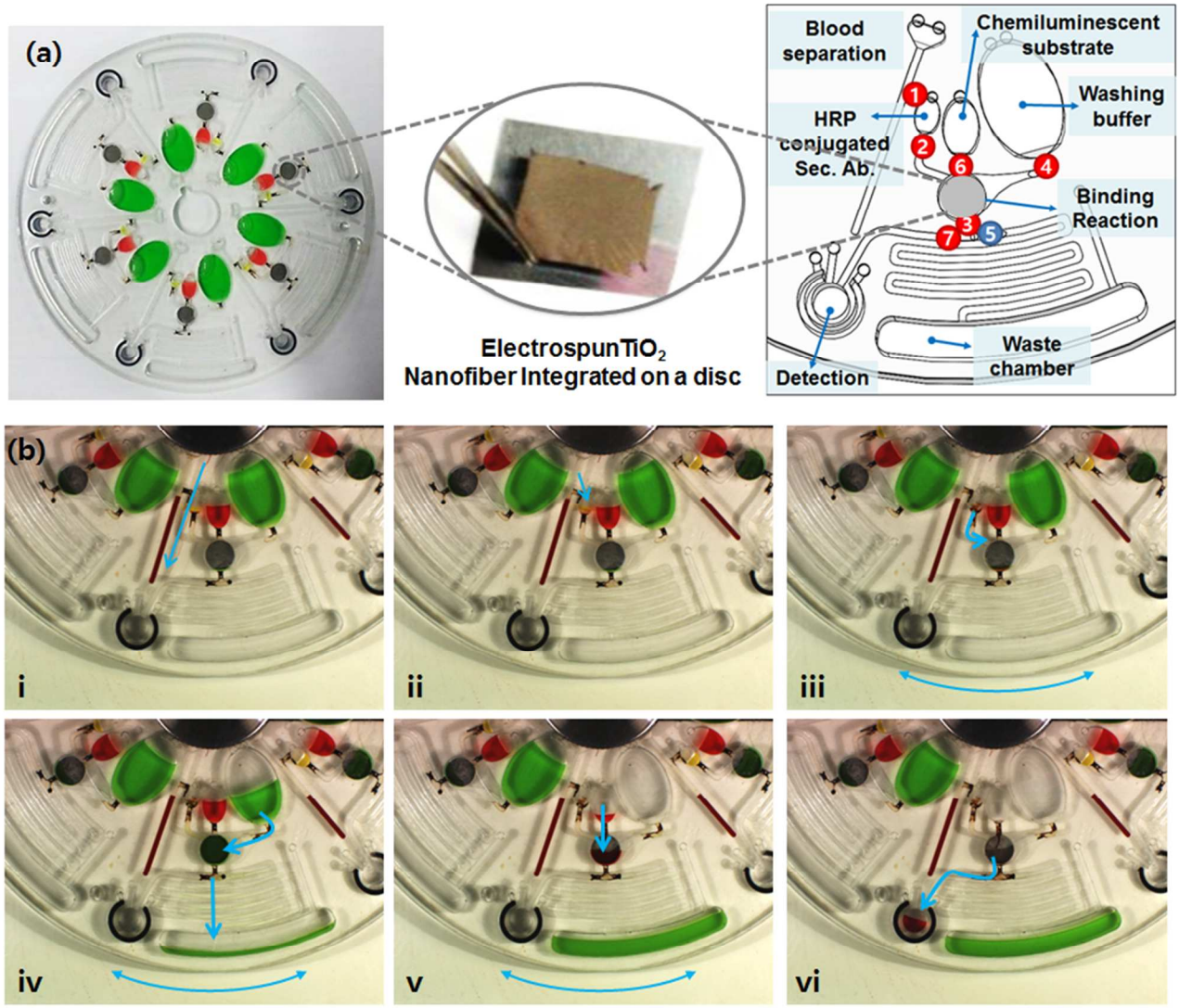

Fig.6 Microfluidic design and operation images of a lab-on-a-disc integrated with a TiO_2 NF mat. (a) Photograph showing the fabricated disc with chambers for the washing buffer, the detection antibodies, the chemiluminescent substrate, and the TiO_2 NFs conjugated with antibodies. Food dyes are used for the washing buffer and substrate for visualization. The red circles with numbers are normally closed laser-irradiated ferrowax microvalves (LIFM), whereas the blue circle with the number 5 is a normally open LIFM. The numbers indicate the order of valve operation. (b) CCD images showing the spinning disc during full operation of the ELISA on a disc. In brief, (i) blood is separated by centrifugal force; (ii) valve #1 is opened, and 4 μL of plasma is transferred to the chamber containing 8 μL of detecting antibodies conjugated with HRP and mixed for 5 s; (iii) the solution is transferred by opening valve #2 to the binding reaction chamber modified with capturing antibodies and incubated for 30 min in a mixing mode, and the residual mixture is removed to the waste chamber by opening valve #3; (iv) the washing buffer is transferred by opening valve #4 to the binding reaction chamber to remove plasma residues and repeated twice, and valve #5 is closed; (v) valve #6 is opened, and the chemiluminescent substrate solution is transferred to the binding reaction chamber and incubated; and (vi) the incubated solution is finally transferred to a detection chamber by opening valve #7 for luminescence intensity measurements.

Cite this: DOI: 10.1039/c0xx00000x

www.rsc.org/xxxxxx

ARTICLE TYPE

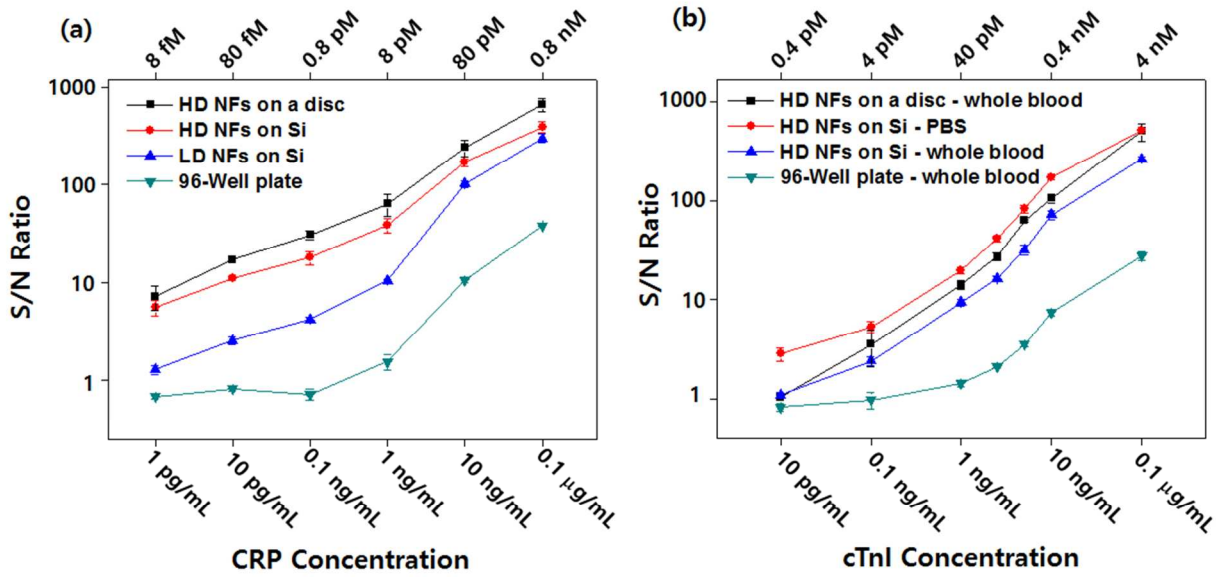

Fig.7 (**a**) Calibration curves for the detection of CRP spiked in a *CRP-free serum* on a 96-well plate, LD TiO_2 NFs assembled on a Si substrate, HD TiO_2 NFs assembled on a Si substrate, and HD TiO_2 NFs assembled on a lab-on-a-disc. (**b**) Calibration curves for the detection of cTnI spiked in *whole blood* or PBS buffer on HD TiO_2 NFs assembled on a Si substrate and for detection of cTnI spiked in whole blood on HD TiO_2 NFs assembled on a lab-on-a-disc and 96-well plate. Error bars indicate the standard deviation of at least three independent measurements.

Acknowledgements

This work was supported by National Research Foundation of Korea (NRF) grants (2013R1A2A2A05004314, 2012-0005090) and a grant from the Korean Health Technology R&D Project, Ministry of Health & Welfare Republic of Korea (A121994), funded by the Korean government.

Notes and references

Department of Biomedical Engineering, School of Life Sciences, Ulsan National Institute of Science and Technology (UNIST), Banyeon-ri 100, Ulsan,689-798, Republic of Korea.E-mail: ykcho@unist.ac.kr Tel: +82 52 217 2511

†Electronic Supplementary Information (ESI) available: Experimental set up for on disc detection system, SEM images, tack test, TEM-EDS and size distribution histogram for the analysis of nanofibers, standard curves for the optimization of capture and detection antibody, calibration curves for the detection of CRP and cTnI, atomic composition of nanofibers, spin program for the immunoassay and a movie file showing the total process of fully automated immunoassay on a disc. See DOI: 10.1039/b000000x/

‡ *These authors contributed equally to this work.*

1. W. Hu and C. M. Li, *Wiley Interdiscip. Rev. Nanomed. Nanobiotechnol.*, 2011, **3**, 119-133.
2. Y. Zhang, Y. Guo, Y. Xianyu, W. Chen, Y. Zhao and X. Jiang, *Adv. Mater.*, 2013, **25**, 3802-3819.
3. R. Baltazar, C. R. Vistas and G. M. Ferreira, *Nanocomposite Particles for Bio-Applications*, Pan Stanford Publishing, 2011, pp. 265-282.
4. P. Roy, S. Berger and P. Schmuki, *Angew. Chem. Int. Ed.*, 2011, **50**, 2904-2939.
5. C. Yang-Kyu and K. Chang-Hoon, *Biosensors and Cancer*, Science Publishers, 2012, pp. 164-183.
6. S. Chantasirichot and K. Ishihara, *Biosens. Bioelectron.*, 2012, **38**, 209-214.
7. D. Yang, X. Niu, Y. Liu, Y. Wang, X. Gu, L. Song, R. Zhao, L. Ma, Y. Shao and X. Jiang, *Adv. Mater.*, 2008, **20**, 4770-4775.
8. N. Zhang, Y. Deng, Q. Tai, B. Cheng, L. Zhao, Q. Shen, R. He, L. Hong, W. Liu, S. Guo, K. Liu, H.-R. Tseng, B. Xiong and X.-Z. Zhao, *Adv. Mater.*, 2012, **24**, 2756-2760.
9. S. Agarwal, J. H. Wendorff and A. Greiner, *Polymer*, 2008, **49**, 5603-5621.
10. B. Ding, M. Wang, X. Wang, J. Yu and G. Sun, *Materials Today*, 2010, **13**, 16-27.
11. W. E. Teo and S. Ramakrishna, *Nanotechnology*, 2006, **17**, R89.
12. P. Kiselev and J. Rosell-Llompart, *J. Appl. Polym. Sci.,* 2012, **125**, 2433-2441.
13. S. J. Lee, R. Tatavarty and M. B. Gu, *Biosens. Bioelectron.*, 2012, **38**, 302-307.
14. P. Kar, A. Pandey, J. J. Greer and K. Shankar, *Lab Chip*, 2012, **12**, 821-828.
15. K. J. Son, S. H. Ahn, J. H. Kim and W.-G. Koh, *ACS Appl. Mater. Interfaces*, 2011, **3**, 573-581.
16. W. Tu, Y. Dong, J. Lei and H. Ju, *Anal. Chem.,* 2010, **82**, 8711-8716.
17. S. Liu and A. Chen, *Langmuir*, 2005, **21**, 8409-8413.
18. D. V. Portan, A. A. Kroustalli, D. D. Deligianni and G. C. Papanicolaou, *J. Biomed. Mater. Res. A*, 2012, **100A**, 2546-2553.

19. M. Dettin, A. Bagno, R. Gambaretto, G. Iucci, M. T. Conconi, N. Tuccitto, A. M. Menti, C. Grandi, C. Di Bello, A. Licciardello and G. Polzonetti, *J. Biomed. Mater. Res. A*, 2009, **90A**, 35-45.
20. W.-J. Kim, S. Kim, B. S. Lee, A. Kim, C. S. Ah, C. Huh, G. Y. Sung and W. S. Yun, *Langmuir*, 2009, **25**, 11692-11697.
21. D. Li and Y. Xia, Nano Lett., 2003, **3**, 555-560.
22. R. Gorkin, J. Park, J. Siegrist, M. Amasia, B. S. Lee, J.-M. Park, J. Kim, H. Kim, M. Madou and Y.-K. Cho, *Lab Chip*, 2010, **10**, 1758-1773.
23. U. Y. Schaff and G. J. Sommer, *Clin. Chem.*, 2011, **57**, 753-761.
24. B. S. Lee, J.-N. Lee, J.-M. Park, J.-G. Lee, S. Kim, Y.-K. Cho and C. Ko, *Lab Chip*, 2009, **9**, 1548-1555.
25. B. S. Lee, Y. U. Lee, H.-S. Kim, T.-H. Kim, J. Park, J.-G. Lee, J. Kim, H. Kim, W. G. Lee and Y.-K. Cho, *Lab Chip*, 2011, **11**, 70-78.
26. J. Park, V. Sunkara, T.-H. Kim, H. Hwang and Y.-K. Cho, *Anal. Chem.*, 2012, **84**, 2133-2140.
27. J.-M. Park, Y.-K. Cho, B.-S. Lee, J.-G. Lee and C. Ko, *Lab Chip*, 2007, **7**, 557-564.
28. R. Zhu, C.-Y. Jiang, X.-Z. Liu, B. Liu, A. Kumar and S. Ramakrishna, *Appl. Phys. Lett.*, 2008, **93**, 013102-013103.
29. M. Y. Song, Y. R. Ahn, S. M. Jo, D. Y. Kim and J.-P. Ahn, *Appl. Phys. Lett.*, 2005, **87**, 113113-113113.
30. O. Katsuhiro, D. Bin, T. Yosuke, N. Takayuki, Y. Michiyo, S. Shinichiro, O. Shingo, Y. Masato and S. Seimei, *Nanotechnology*, 2006, **17**, 1026.